by only one-fifth of the amount of O_2 used. Thus the concentration of O_2 in the submerged organs decreases continuously in darkness while that of N_2 increases, leading to a depression of the respiratory rate and a steady decline in the rate of air intake. As the concentration of O_2 inside the plant drops with increasing length of the dark period, the diffusional component of O_2 movement into the plant must increase (*9*).

Both surfaces of the submerged rice leaf are separated from the water by continuous air layers, the volume of which reaches 44 percent of that of the leaf (*6*). The role of air layers in the transport of gases from the atmosphere into the internal air passages is illustrated in Fig. 4. A single leaf protruding 6 cm from the water into the leaf chamber drew air from the atmosphere at the rate of 7.2 ml/hour (Fig. 4A). After 60 minutes both sides of this leaf were covered from the tip to a point 1 cm above the water with transparent nail polish to block the stomatal pores. At the same time, a 5-mm-wide ring of nail polish was painted on the leaf blade 14 cm below the water surface to interrupt the continuity of the air layers and to demonstrate that nail polish did not interfere with air conductance inside the leaf. The rate of air flow into the plant was not affected by these treatments (Fig. 4B). Withdrawal of air by the leaf caused the water level in the leaf chamber to rise. When the water level reached the area of the leaf blade that was covered with nail polish, the entrance to the air layers closed. This resulted in immediate and complete cessation of air intake (Fig. 4C). After the water level in the chamber was lowered to open the entrance to the air layers, the original rate of air intake was restored (Fig. 4D). The importance of the air layers was shown by the experiment represented in Fig. 4E. When another 5-mm-wide ring of nail polish was painted on the leaf just below the water surface so that the entrance to the air layers was blocked and only 1 cm of uncovered leaf remained above the water, the rate of air intake was reduced 12-fold (*10*). These results indicate that air from the atmosphere is drawn into the air layers and then passes into the internal air passages via the stomata, provided that a small portion of the leaf protrudes from the water and the entrance to the air layers is open. Air layers greatly decrease the leaf area that must be kept above the water to replace O_2 consumed in respiration and are essential under conditions of high flooding.

We know of only one other report of aeration in an aquatic plant, the water lily, proceeding by mass flow (*11*). In that case it was suggested that the movement of air is caused by thermal transpiration and hygrometric pressurization. Such a system of aeration could not operate in darkness, when the availability of O_2 inside the plant is particularly restricted. The mechanism of aeration that we propose for partially submerged rice plants is driven by solubilization of respiratory CO_2 in water. It functions in light as well as darkness and may also operate in other semiaquatic plants.

ILYA RASKIN*
HANS KENDE
MSU-DOE Plant Research Laboratory, Michigan State University, East Lansing 48824

References and Notes

1. S. K. De Datta, *Principles and Practices of Rice Production* (Wiley, New York, 1981), pp. 247–251; B. S. Vergara, B. Jackson, S. K. De Datta, in *Climate and Rice* (International Rice Research Institute, Los Baños, Philippines, 1976), pp. 301–319.
2. W. Armstrong, in *Plant Life in Anaerobic Environments*, D. D. Hook and R. M. M. Crawford, Eds. (Ann Arbor Science, Ann Arbor, Mich., 1978), pp. 269–297.
3. W. Armstrong, *Adv. Bot. Res.* **7**, 225 (1979); D. A. Barber, M. Ebert, N. T. S. Evans, *J. Exp. Bot.* **13**, 397 (1962); D. J. Greenwood, *New Phytol.* **66**, 337 (1967).
4. P. B. Kaufman, *Phytomorphology* **9**, 277 (1959).
5. C. D. John, *Plant Soil* **47**, 269 (1977).
6. I. Raskin and H. Kende, *Plant Physiol.* **72**, 447 (1983).
7. Mass flow of air into rice plants was also demonstrated by the following experiment. A rice plant was partially submerged and all tillers except two were cut off below the water surface. The remaining two culms with leaves attached were trimmed to 7 cm above the water surface. They were enclosed in an inverted 30-ml syringe that was lowered into the water such that a 25-ml headspace of air remained above the two culms. The syringe was sealed with a serum-vial cap through which gas samples could be taken for O_2 analysis by gas chromatography. A rising water level inside the syringe indicated uptake of air by the plant. In light the plant took up 20 ml of air in 2 hours. The concentration of O_2 in the remaining 5 ml of headspace was unchanged (21 percent).
8. From four experiments in which we measured air uptake by illuminated plants with and without roots, we estimated that gas uptake by roots, 100 to 120 cm under water, was on the order of 4 ml/hour. Diffusion of O_2 over this distance could have contributed but a small fraction of the gas taken up by the roots. This was calculated from the equation for the diffusion of gases through a tubular structure (*2*), according to which the rate of diffusion is equal to $[DA\ (C_2 - C_1)]/L$, where D is the diffusion coefficient of O_2 in air, A is the cross-sectional area of the tube, C_2 is the concentration of O_2 at the source, C_1 is the concentration of O_2 at the sink, and L is the length of the diffusion path. The combined cross-sectional area of the air layers and of the internal air spaces of six leaves protruding into the leaf chamber of the volumetric setup is 0.08 cm^2 (*6, 13*). On the basis of the diffusion equation, the rate of diffusion of O_2 from a source containing 21 percent O_2 to a sink containing 0 percent O_2 through a 100-cm-long tube with a cross-sectional area of 0.08 cm^2 would be 0.12 ml/hour. This value is an overestimate for the diffusion of O_2 from the atmosphere to the roots of a rice plant 100 cm below the surface because the diffusion equation does not take into account the diffusional resistances in the plant.
9. The volume of air taken up by a partly submerged rice plant is of the same magnitude as the volume of O_2 consumed during respiration. The average dry weight of the shoot of a rice plant used in our experiments was 6.4 g and that of the root 1.0 g. Using these dry weight determinations and published respiration rates of rice roots and leaves (*14*), we have calculated an average respiratory rate of 3.8 ml of O_2 per hour for the root and 14.7 ml/hour for the shoot. In the experiment represented in Fig. 2, the initial rate of air intake in darkness was 17.7 ml/hour, or very close to the estimated respiratory rate of a whole plant.
10. If less than 15 cm^2 of a leaf with blocked air layers remained above the water, the air layers decreased in size until, after several hours, water was drawn into the plant infiltrating the air spaces. This demonstrates that a significant negative pressure will develop inside the air-conducting spaces of the plant when its access to air is restricted.
11. J. W. H. Dacey, *Science* **210**, 1017 (1980).
12. J.-P. Métraux and H. Kende, *Plant Physiol.* **72**, 441 (1983).
13. I. Raskin, *HortScience* **18**, 698 (1983).
14. K. Tajima, *Proc. Crop Sci. Soc. Jpn.* **33**, 371 (1965).
15. We thank R. deZacks for assistance in growing the plants and N. E. Good, A. D. Hanson, and Y. Vaadia for helpful discussions. Supported by National Science Foundation grant PCM 81-09764 and Department of Energy contract DE-AC02-76ER0-1338.
* Present address: Shell Development Company, P.O. Box 4248, Modesto, Calif. 95352.

12 September 1984; accepted 10 December 1984

Construction and Recovery of Viable Retroviral Genomes Carrying a Bacterial Suppressor Transfer RNA Gene

Abstract. *The integration of retroviral genomes into cellular DNA can induce mutations by altering the expression of nearby cellular genes and can serve to identify the gene affected. The construction of a retrovirus that stably carries a suppressor transfer RNA gene from* Escherichia coli *has allowed facile recovery of the viral genome in vectors marked with amber mutations. This virus can be used for rapid isolation of cellular sequences at the site of proviral insertion.*

Retroviruses are unique among viruses of vertebrates in that a DNA copy of the viral genome integrates into the host genome as an obligate step in the life cycle. This integration event often affects the expression of host genes near the site of the insertion (*1–4*). The insertions can be useful in identifying and cloning the affected host genes because the new provirus can be used as a hybridization probe for this region of the host genome.

One difficulty in identifying new provirus insertions in mouse cells is the presence of endogenous sequences with homology to the exogenous viral DNA (*5*). These sequences obscure the presence of the newly inserted viral DNA in hybridization experiments, even though probes with less homology to the endog-

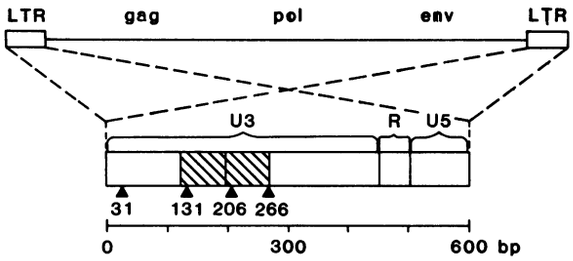

Fig. 1. Positions of the four insertions of the SuIII gene in the long terminal repeat of Moloney murine leukemia virus. The complete viral genome and an enlargement of the LTR's are shown. The 75-bp enhancer regions are shaded.

enous sequences have been prepared (*6*). To overcome these difficulties, we constructed replication-competent variants of a murine leukemia virus that carry an inserted DNA sequence. Because the inserted DNA expresses a functional suppressor transfer RNA (tRNA) in bacteria, we can select recombinant clones containing proviral DNA (*7*) by using the Charon series vectors (*8*) with amber mutations in essential phage genes. Alternatively, the insert can be detected by hybridization procedures, because mammalian cells contain no sequences homologous to the prokaryotic gene.

We constructed the new viral genomes from selected linker insertion mutants (*9*) of Moloney murine leukemia virus (M-MuLV). A 220-base-pair (bp) Eco RI fragment containing the SuIII tyrosine suppressor tRNA gene from the plasmid piVX (*10*) was inserted into the new Eco RI site of these genomes. One insertion was made near the left edge of the viral long terminal repeat (LTR), whereas the other was made in one (the 5′ proximal one) of the two 75-bp tandem repeats with transcriptional enhancer activity (*11*). Two additional variants were generated by the direct insertion of the SuIII gene into Sau96 I sites of wild-type M-MuLV; these insertions were mapped into the 75-bp enhancer elements on the 3′ side (Table 1 and Fig. 1). The orientation of the SuIII gene relative to the viral genome was not determined.

To assess the effects of these insertion mutations on the replication of the viruses in mouse cells we introduced each mutant DNA into NIH 3T3 cells with the use of DEAE-Dextran (*12*). Constructs formed from nonpermuted clones were applied directly to the cells; those formed from permuted clones were excised from the plasmid vector and oligomerized to form an infectious structure (*13*). All four DNA's induced the same number of XC syncytial plaques per microgram of DNA as were induced by the parental linker insertion mutants and by the wild type (Table 1). Recipient cultures were passaged for 2 weeks, and the supernatant media from the cultures were assayed for virion-associated reverse transcriptase (*14*). Each culture showed the same high level of reverse transcriptase as did the wild-type infected cells. Thus, by both criteria the viruses were still replication competent.

The insertions were made in such a way that the SuIII gene should have been retained in both copies of the viral LTR throughout the replication cycle. However, some linker insertion mutations were unstable (*9*) and could be lost upon viral passage. To test for instability, we analyzed the structures of two viral genomes after allowing spread through the recipient cultures for 1 month. Virus from the recipient cells was used to infect fresh NIH 3T3 cells at a high multiplicity, and after 24 hours the unintegrated proviral DNA was isolated by the Hirt procedure (*15*). The DNA's were analyzed by blot hybridization (*16*) (Fig. 2). Mutant in31SuIII proved to be completely stable; all of the viral DNA's were 200 bp larger than the wild-type DNA, and their LTR's contained Eco RI sites. The other mutant, in131SuIII, showed evidence of instability. In addition to the expected mutant genome, a second species was present that was close to the wild type in size and was resistant to cleavage by Eco RI (Fig. 2). Mutant in131SuIII thus appeared to give rise to variants without the insert.

One explanation for the instability of mutant in131SuIII was suggested by the position of the insertion in one of the two 75-bp repeated sequences in the LTR; the sequence could be excised from the virus by homologous recombination between the two repeats. The result would be a virus carrying only one copy of the repeat. To test whether this was the mechanism of loss, we measured more accurately the length of the LTR regions of the in131SuIII DNA's by cleavage with Pvu I (Fig. 2D). Wild-type DNA released a fragment of length 0.9-kilobase (kb) from the left end of the genome. Mutant in131SuIII virus released two fragments; one was larger

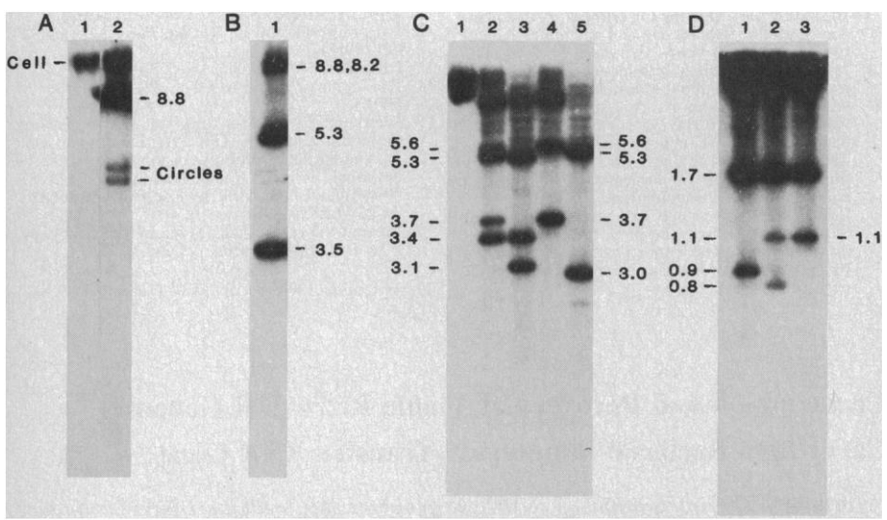

Fig. 2. Southern blot hybridizations of preintegrative viral DNA's synthesized after infection of NIH 3T3 cells. (A) (Lane 1) Uninfected cells; hybridization detects only the endogenous viral sequences in host DNA. (Lane 2) Wild-type virus; the full-length linears and two circular species can be seen. (B) Wild-type DNA's after cleavage with Hind III plus Eco RI; the linear form was cut to two subgenomic fragments, and the circular DNA's were cut to full-length linear forms. (C) Mutant DNA's cut with various enzymes. (Lane 1) Uninfected cells. (Lane 2) in131SuIII viral DNA cut with Hind III alone; the linear DNA was cut to four fragments—two from viral DNA carrying the suppressor gene (5.6 and 3.7 kb) and two from virus that had lost the insert (5.3 and 3.4 kb). (Lane 3) in131SuIII DNA's cut with Hind III plus Eco RI; only the fragments from the larger virus seen in lane 2 were sensitive to Eco RI—the smaller virus fragments were resistant. (Lane 4) in31SuIII viral DNA cut with Hind III alone; the viral genome was completely homogeneous and showed stable retention of the inserted DNA. (Lane 5) in31SuIII cut with Hind III plus Eco RI; both DNA termini were completely cleaved by Eco RI. (D) Mutant DNA's cut with Pvu I. (Lane 1) Wild-type viral DNA; the fragment migrating at 0.9 kb contains the 5′ end of the genome (*20*). (Lane 2) in131SuIII DNA; two 5′ end fragments were produced—one larger than wild type by about 200 bp, indicative of the insertion, and one smaller by about 75 bp, indicating simultaneous loss of the insertion and one of the repeated enhancer elements. (Lane 3) in31SuIII DNA; a single 5′ end fragment larger than wild type was produced, again indicating complete retention of the insertion.

than the wild type by about 200 bp, and the other was smaller than the wild type by about 75 bp. Thus, the loss of the insert was associated with a loss of 75 additional base pairs, consistent with loss of one of the two repeats. The stable mutant, in31SuIII, showed only the larger DNA fragment as expected, suggesting that insertions into the retroviral genome are not inherently unstable unless flanked by homologous sequences.

To test whether the suppressor gene was still functional after replication in mammalian cells, we cloned preintegrative proviral DNA by selection for the function of the SuIII tRNA. Low molecular weight DNA was isolated from NIH 3T3 cells soon after infection with mutant in131SuIII, cleaved with Sac I, and cloned in Charon 16A, a phage vector with amber mutations in the A and B genes (*8*). The resulting phages were titered either on host LE392, an amber suppressing strain that permits the growth of all recombinants, or on host W3110, a nonsuppressing host that will plate only amber phages carrying their own suppressor gene. Of the 10^4 recombinant phages capable of being plated on LE392, three phages were able to grow on W3110. This frequency is in good accord with the relative abundance of viral DNA in the preparations. Restriction analysis of these phage DNA's revealed that each contained the expected fragment of viral DNA (Fig. 3A). Thus, the viral genome could be quickly cloned by genetic selection without the need for screening by hybridization.

To test whether the viral genome could be recovered after integration into cellular DNA, we prepared cell lines with many integrated proviruses. NIH 3T3 cells producing mutant in131SuIII were treated with mitomycin C (10 μg/ml) for 4 hours and then cocultivated for 3 days with undifferentiated F9 teratocarcinoma cells (*17*). Cells carrying as many as 100 proviruses were recovered (*18, 19*) because these cells do not express viral proteins and so do not exhibit superinfection exclusion (*20*). Three cloned teratocarcinoma cell lines were isolated from this population, and genomic DNA's from each line were cleaved with Bam HI and cloned in the phage vector Charon 30A. The resulting genomic DNA libraries were amplified in Le392 and then plated on the nonsuppressing lacZ$^-$ amber host LG75 in the presence of IPTG (isopropyl-β-D-thiogalactopyranoside) and the indicator X-Gal (5-bromo-4-chloro-3-indolyl-β-D-galactoside) (*21*). In each amplified library, between 50 and 100 phages of a total of 10^6 phages that grew on LE392 yielded blue plaques on LG75. These phages were able to suppress the amber mutations they carried, as well as the lacZ$^-$ amber mutations in the host, and should therefore contain cloned portions of the integrated viral genome. Hybridization analysis of these phages confirmed this expectation (Fig. 3B). Thus, we could rapidly isolate integrated proviral DNA's from infected cells by selection for the SuIII gene.

Table 1. Properties of mutant genomes. Abbreviations: XC, plaque formation after XC overlay, with + indicating 500 to 1000 plaque-forming units per 100 ng of DNA; RT, release of reverse transcriptase by infected cell lines; N.D., not done. For a discussion of parent DNA's, see (*9*).

Mutant	Parent DNA	Site of insertion	Position of insertion	XC[a]	RT[b]	Stability
in31SuIII	pT11	Alu I	Nucleotide 31	+	+	+
in131SuIII	pa8.2	Hae III	Nucleotide 131	+	+	+/−
in206SuIII	pT11	Sau96 I	Nucleotide 206	+	+	N.D.
in266SuIII	pT11	Sau96 I	Nucleotide 266	+	+	N.D.

It should be possible to select for the inactivation of a gene of interest mediated by proviral insertion and then to isolate the gene by isolation of the provirus. Viral genomes carrying selectable markers such as those we have described would facilitate such efforts because clones could be isolated without interference caused by the presence of homologous sequences in the host genome and without the need for laborious screening procedures. We demonstrated the feasibility of this scheme by cloning integrated proviruses that had inactivated the host gene encoding hypoxanthine-guanine phophoribosyltransferase by insertion into the gene (*22*).

A finding implicit in these results is that M-MuLV can tolerate major alterations in the viral LTR without deleterious effects on the viral life cycle. The insertion of the suppressor gene into in31SuIII 30 bp from the 5′ edge of the viral LTR does not prevent the integration of the virus into the host genome (data not shown). Furthermore, the mutants demonstrate that one intact enhancer is sufficient for normal replication, in accord with the viability of natural variants carrying only one enhancer (*23*). Finally, as all of the mutants demonstrate, the total size of the viral LTR is not invariant; 220 bp can be added to the original 589 bp without grossly affecting any step in viral replication.

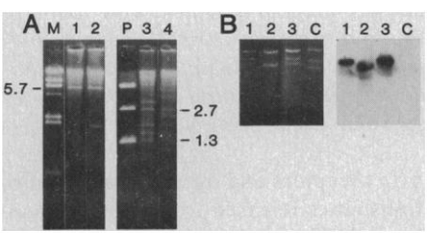

Fig. 3. Agarose gel electrophoresis of phage DNA's containing viral genomes isolated by selection for the suppressor tRNA gene. (A) Analysis of Charon 16A clones prepared from Sac I fragments of preintegrative viral DNA's. (Lane M) Marker DNA's; the sizes from top to bottom are 23.1, 9.4, 6.6, 4.4, 2.3, 2.0, and 0.56 kb. (Lane P) A control plasmid DNA containing the M-MuLV genome cleaved with Kpn I. DNA's from two independent phages cleaved with Sac I (lanes 1 and 2) or Kpn I (lanes 3 and 4) show the fragments expected from the viral restriction map (arrows). One phage contains an extra DNA fragment. (B) Analysis of proviral clones prepared from integrated viral DNA's. DNA from cells infected with in131SuIII virus was cleaved with Bam HI and cloned in Charon 30A. (Lanes 1 to 3) DNA's of three independent SuIII$^+$ phages cleaved with Bam HI. (Lane C) DNA of the Charon 30A vector cleaved with Bam HI. The left panel shows the ethidium fluorescence of the stained gel and the right panel shows the autoradiogram of the blotted DNA after hybridization to radioactive viral DNA probe.

LESLIE I. LOBEL
Department of Biochemistry and Molecular Biophysics, Columbia University College of Physicians and Surgeons, New York 10032
MAYURI PATEL
WALTER KING
M. CHI NGUYEN-HUU
Departments of Microbiology and Urology, Columbia University
STEPHEN P. GOFF
Department of Biochemistry, Columbia University

References and Notes

1. B. G. Neel, W. S. Hayward, H. L. Robinson, J. Fang, S. M. Astrin, *Cell* **23**, 323 (1981); W. S. Hayward, B. G. Neel, S. M. Astrin, *Nature (London)* **290**, 475 (1981); G. S. Payne, J. M. Bishop, H. E. Varmus, *ibid.* **295**, 209 (1982).
2. Y.-K. T. Fung, W. G. Lewis, L. B. Crittenden, H.-J. Kung, *Cell* **33**, 357 (1983).
3. R. Nusse and H. E. Varmus, *ibid.* **31**, 99 (1982); P. R. Etkind and N. H. Sarkar, *J. Virol.* **45**, 114 (1983); G. Peters, S. Brookes, R. Smith, C. Dickson, *Cell* **33**, 369 (1983).
4. H. E. Varmus, N. Quintell, S. Oritz, *Cell* **25**, 23 (1981); N. A. Jenkins, N. G. Copeland, B. A. Taylor, B. K. Lee, *Nature (London)* **293**, 370 (1981); D. Wolf, V. Rotter, *Mol. Cell Biol.* **4**, 1402 (1984); A. Schnieke, K. Harbers, R. Jaenisch, *Nature (London)* **304**, 315 (1983).
5. For an extensive review, see J. Coffin, *RNA Tumor Viruses*, R. Weiss, N. Teich, H. Varmus, J. Coffin, Eds. (Cold Spring Harbor Laboratory, Cold Spring Harbor, N.Y., 1982), pp. 1109–1204; primary references include: L. D. Gelb *et al.*, *Nature (London)* **244**, 76 (1973); S. K. Chattopadhyay *et al.*, *Proc. Natl. Acad. Sci. U.S.A.* **72**, 906 (1975); S. K. Chattopadhyay *et al.*, *ibid.* **77**, 5774 (1980); S. K. Chattopadhyay *et*

al., *Virology* **113**, 465 (1981); D. Steffen and R. A. Weinberg, *Cell* **15**, 1003 (1978); D. Steffen *et al.*, *Proc. Natl. Acad. Sci. U.S.A.* **76**, 4554 (1979); N. A. Jenkins *et al.*, *J. Virol.* **43**, 26 (1982).
6. I. M. Verma, personal communication.
7. M. P. Goldfarb, K. Shimizu, M. Perucho, M. Wigler, *Nature (London)* **296**, 404 (1982); K. Shimizu, M. Goldfarb, M. Perucho, M. Wigler, *Proc. Natl. Acad. Sci. U.S.A.* **80**, 383 (1983).
8. D. L. Rimm, D. Horness, J. Kucera, F. R. Blattner, *Gene* **12**, 301 (1980); B. G. Williams and F. R. Blattner, *J. Virol.* **29**, 555 (1979).
9. L. I. Lobel and S. P. Goff, *Proc. Natl. Acad. Sci. U.S.A.* **81**, 4149 (1984).
10. B. Seed and T. Maniatis, personal communication [noted in *Molecular Cloning*, T. Maniatis, E. F. Fritsch, J. Sambrook, Eds. (Cold Spring Harbor Laboratory, Cold Spring Harbor, N.Y., 1980)].
11. B. Levinson, G. Khoury, G. Vande Woude, P. Gruss, *Nature (London)* **295**, 568 (1982).
12. J. H. McCutchan and J. S. Pagano, *J. Natl. Cancer Inst.* **41**, 351 (1968).
13. P. Schwartzberg, J. Colicelli, S. P. Goff, *J. Virol.* **46**, 538 (1983); P. Schwartzberg, J. Colicelli, M. L. Gordon, S. P. Goff, *ibid.* **49**, 918 (1984); P. Schwartzberg, J. Colicelli, S. P. Goff, *Cell* **37**, 1043 (1984).
14. S. P. Goff, P. Traktman, D. Baltimore, *J. Virol.* **38**, 239 (1981).
15. B. Hirt, *J. Mol. Biol.* **26**, 365 (1967).
16. E. M. Southern, *ibid.* **98**, 503 (1975).
17. E. G. Bernstine *et al.*, *Proc. Natl. Acad. Sci. U.S.A.* **70**, 3899 (1973).
18. C. L. Stewart *et al.*, *ibid.* **79**, 4098 (1982).
19. W. King and M. C. Nguyen-Huu, unpublished data.
20. P. S. Sarma *et al.*, *Virology* **33**, 180 (1967).
21. J. H. Miller, in *Experiments in Molecular Genetics* (Cold Spring Harbor Laboratory, Cold Spring Harbor, N.Y., 1972).
22. W. King, M. D. Patel, L. I. Lobel, S. P. Goff, C. C. Nguyen-Huu, *Science*, in press.
23. C. Van Beveren, E. Rands, S. K. Chattopadhyay, D. R. Lowy, I. M. Verma, *J. Virol.* **41**, 542 (1982); J. G. Sutcliffe *et al.*, *Proc. Natl. Acad. Sci. U.S.A.* **77**, 3302 (1980); C. Van Beveren *et al.*, *ibid.*, p. 3307.
24. We thank J. Van Oostrum for gifts of DNA ligase. Supported by PHS grant 2 P30 CA 23767 awarded by the NCI to S.P.G. and R01 CA 37176 to C.N.-H. Additional support was provided to S.P.G. by the Hirschl Trust and by the Searle Foundation and to M.C.N.-H. by the National Cancer Cytology Center.

22 October 1984; accepted 9 January 1985

Silver-Intensified Gold and Peroxidase as Dual Ultrastructural Immunolabels for Pre- and Postsynaptic Neurotransmitters

Abstract. *An ultrastructural immunostaining method that uses silver-intensified gold was combined with another procedure that uses biotin peroxidase conjugates to allow simultaneous identification of two neurotransmitter-related antigens in the central nervous system. Tyrosine hydroxylase–immunoreactive neurons labeled with silver-intensified gold could be differentiated at both light and electron microscopic levels from glutamate decarboxylase–immunoreactive neurons labeled with peroxidase. Cross reactivity of the second group of immunoreagents with the first group was reduced by the heavy metal silver shell formed around the colloidal gold immunoglobulin complex. With this dual pre-embedding method, peroxidase-stained axons containing the inhibitory neurotransmitter γ-aminobutyric acid were found to synapse directly on silver-stained dopamine neurons in the rat dorsomedial hypothalamus. This approach can be used in combination with a post-embedding immunocytochemical colloidal gold procedure, allowing ultrastructural identification of three neurotransmitter-related antigens in the same tissue section.*

The primary function of neurons may be considered to be one of intercellular electrochemical communication and information processing, generally occurring through the release of one (or more) of 30 to 50 different neuroactive substances, loosely termed neurotransmitters. The electrical response of a postsynaptic cell is determined both by its own receptors and by the type of neurotransmitter released from the presynaptic cell. The complexity of connections in the central nervous system is bewildering, particularly in nonlaminated areas like the hypothalamus, where obvious morphological clues to cell type may be absent. Studies based on immunocytochemical identification of a single primary antiserum against a neurotransmitter-related antigen have proved useful in delineating previously unrecognized neuronal systems. The possibility of identifying and differentially labeling both the presynaptic and postsynaptic elements in the same histological section would allow a more specific characterization of both the biochemistry and the physical circuitry in any area of the brain. Such an analysis of neuronal relations must be based on ultrastructural confirmation of synaptic interaction.

Three objectives may be considered in dual ultrastructural identification of two antigens. (i) The final markers must be readily seen and discriminated from each other with both light and electron microscopy. (ii) Antibody cross-reaction between the series of reagents used to identify two different primary antiserums must be minimized. (iii) Both methods should be sensitive enough to detect low antigen concentrations. Pre-embedding immunostaining with peroxidase followed by post-embedding staining with colloidal gold has been successfully used for dual ultrastructural immunocytochemistry with combinations of cytoplasmic antigens, such as tyrosine hydroxylase (TH), the synthesizing enzyme for catecholamine neurotransmitters, or glutamate decarboxylase (GAD), the synthesizing enzyme for the inhibitory transmitter γ-aminobutyric acid (GABA), together with vesicular antigens such as neurophysin (*1–3*); as this pre-embedding/post-embedding method may work poorly with two cytoplasmic antigens, a different approach was needed for dual identification of GAD and TH.

Although gold particles can be used without intensification for immunocytochemical staining for light microscopy (*4*), significant membrane damage must occur to achieve penetration of gold particles large enough to see (20 to 40 nm); even then the resultant pinkish immunostaining can be faint. One purpose of this study was to find a simple intensification procedure compatible with reasonable ultrastructural preservation. Ideally, the technique should work with the smallest gold particles available, thus reducing the severity of membrane damage necessary for tissue penetration. Finally, the procedure should be compatible with, yet differentiable from, other ultrastructural immunostaining markers, particularly horseradish peroxidase, to allow for identification of two antigens on the same thin electron microspic section. Various methods of intensification of many different metals including silver, cobalt, osmium, and gold have been described (*5, 6*).

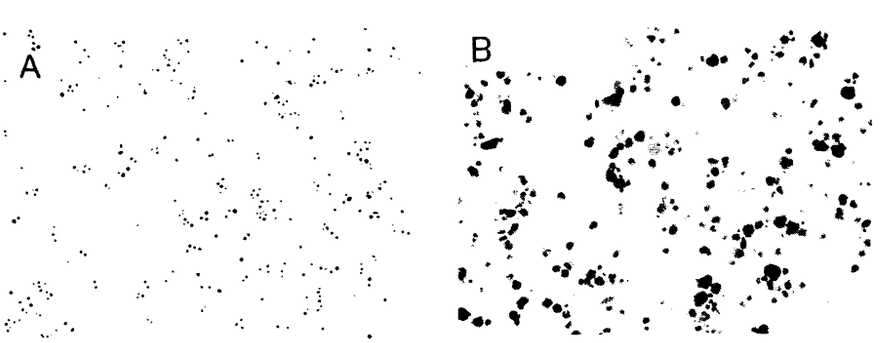

Fig. 1. Effect of intensification on colloidal gold size. (A) Colloidal gold particles (5 nm). (B) Gold (5 nm) intensified for 20 minutes on a Formvar-coated slot grid. Intensification is influenced by the intensity of ambient light, reagent concentration, agitation, and incubation time in the silver solution.